AlCl₃-Saturated Ionic Liquid Anolyte with an Excess of AlCl₃ for Al–Graphite Dual-Ion Batteries

Shutao Wang,[a, b, c] Maksym V. Kovalenko,*[a, b] and Kostiantyn V. Kravchyk*[a, b]

Al–graphite dual-ion batteries (AGDIBs) represent a compelling battery concept for large-scale stationary storage of electricity in view of their safety, low cost, long cycling life, and high energy efficiency (80–90%). However, at present, the deployment of AGDIBs is intrinsically limited by their low cell-level energy density as a result of the non-rocking-chair operation principle and, consequently, the need for large quantities of acidic chloroaluminate ionic liquid (IL) anolytes as a reservoir of $Al_2Cl_7^-$ ions required for AGDIB operation. Thus far, AGDIBs have commonly employed IL anolytes with moderate acidity (AlCl₃/Lewis base molar ratio of 1.3), which corresponds to charge-storage anolyte capacity of ca. 19 mAh g⁻¹, eventually resulting in low cell-level energy densities of 20–30 Wh kg⁻¹. In this work, we present an AGDIB utilizing an AlCl₃-saturated IL anolyte, containing an excess of AlCl₃ powder for maintaining constant acidity during operation, leading to a theoretical capacity of 52 mAh g⁻¹. The resultant AGDIB possesses an energy density of 59.1 Wh kg⁻¹, along with a high energy efficiency of 85% and an average discharge voltage of 1.71 V.

In a search for inexpensive, large-scale stationary storage of electricity, non-aqueous Al-graphite dual-ion batteries (AGDIBs) have attracted recently much attention due to the high natural abundances of their primary constituents, the long cycle life of up to a quarter of a million cycles, the high energy efficiency of 80–90% and facile manufacturing.[1–8] While recent research efforts on AGDIBs have been mainly focused on the judicious selection of carbonaceous cathode materials, leading to the most notable advances in the performance of AGDIBs,[9–27] the major challenge with such batteries is that they lag behind Li-ion batteries in theoretical cell-level energy density. As described below in detail, we estimate the energy density limit for widely used chloroaluminate ionic liquid (IL) anolyte–cathode combinations to be ca. 30–35 Wh kg⁻¹ at the cell level, which is ten times lower than that of conventional Li-ion systems. The low-energy density of AGDIBs is rooted in their non-rocking-chair operation mechanism, as the large mass of chloroaluminate IL anolyte, being a reservoir of $Al_2Cl_7^-$ ions that are required for the battery operation has to be factored into the energy density calculations. In contrast, a minimal electrolyte amount is needed in rocking-chair type metal-ion batteries, merely to provide an ionic connection between the electrodes.[28,29] Therefore, the most promising avenue for increasing the energy density of ADIBs is to maximize the capacity of the anolyte without compromising the charge storage capacities of the electrodes and the voltage of the battery.

In typical anolytes used for AGDIBs, only $Al_2Cl_7^-$ ions enable the aluminum electroplating, which occurs, consequently, in acidic chloroaluminate melts (i.e., the molar ratio (r) of AlCl₃ to EMIMCl > 1).[30,31] Hence the specific charge-storage capacity of the acidic melts is a function of the $Al_2Cl_7^-$ ion concentration in the ionic liquid. Towards getting an increased charge-storage capacity of anolytes, in this work, we present an AlDIB concept using an AlCl₃-saturated AlCl₃/EMIMCl (1-ethyl-3-methylimidazolium chloride) anolyte with an excess of AlCl₃ powder ($r = 2.1$) for keeping constant acidity during AlDIB charging (Figure 1). The studied anolyte exhibits a high theoretical capacity of 52 mAh g⁻¹ owing to the increased content of the

[a] Dr. S. Wang, Prof. M. V. Kovalenko, Dr. K. V. Kravchyk
     Laboratory of Inorganic Chemistry, Department of Chemistry and Applied
     Biosciences, ETH Zürich
     Vladimir-Prelog-Weg 1, 8093 Zürich, Switzerland
     E-mail: mvkovalenko@ethz.ch
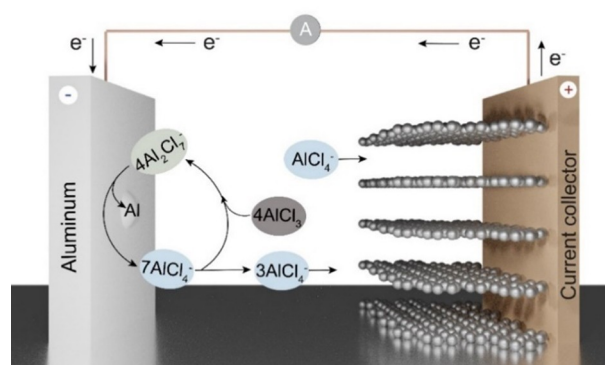   kravchyk@inorg.chem.ethz.ch
[b] Dr. S. Wang, Prof. M. V. Kovalenko, Dr. K. V. Kravchyk
     Laboratory for Thin Films and Photovoltaics
     Empa – Swiss Federal Laboratories for Materials Science and Technology
     Überlandstrasse 129, 8600 Dübendorf, Switzerland
[c] Dr. S. Wang
     Present Address: Department of Chemistry, University College London, 20
     Gordon Street, London, WC1H 0AJ, United Kingdom

An invited contribution to a joint Special Collection between ChemElectroChem and Batteries & Supercaps dedicated to research Beyond Lithium-Ion Batteries

Figure 1. Schematic of the charging process of AGDIB comprising AlCl₃-saturated anolyte with an excess of AlCl₃.

$Al_2Cl_7^-$ ions required for electrodeposition of Al during AGDIB charging. The resulting theoretical energy density of AGDIB comprising $AlCl_3$-saturated anolyte was estimated at the level of 59 Wh kg^{-1}, as follows from the anolyte and graphite cathode capacities of 52 and 103 mAh g^{-1}, respectively, and an average discharge voltage of 1.71 V.

Chloroaluminate Ionic Liquids as an Anolytes for AGDIBs

Generally, chloroaluminate ionic liquids are defined as mixtures of $AlCl_3$ and other Cl^- based salts such as, for instance, commonly used 1-ethyl-3-methylimidazolium chloride (EMIM). The mixture turns liquid at room temperature because of the acid-base reaction between $AlCl_3$ (Lewis acid) and Cl^- (Lewis base), yielding $AlCl_4^-$ anions charge-balanced with, for example, EMIM$^+$ cations. The excess of $AlCl_3$ over EMIMCl results in the formation of acidic ionic liquid formulations containing $Al_2Cl_7^-$. Aluminum electrodeposition from chloroaluminate ionic liquids has been comprehensively studied in the past, leading to the conclusion that solely $Al_2Cl_7^-$ anions (not $AlCl_4^-$) allows the electroplating of Al.[32–41] Consequently, aluminum does not plate from neutral/basic melts (equal/excess molar amount of EMIMCl to $AlCl_3$). Hence the concentration of $Al_2Cl_7^-$ ions in chloroaluminate IL must be proportional to the capacity of the graphite. Specifically, for four $Al_2Cl_7^-$ ions that are reduced at the negative electrode, three $AlCl_4^-$ anions concomitantly intercalate into the graphite positive electrode. The charging of AGDIB stops when there are only $AlCl_4^-$ ions left in the chloroaluminate IL, that correspond to the neutral melt formulation ($AlCl_3$/EMIMCl = 1), or when the maximum capacity of the graphite cathode is reached. In this context, hypothetically, any current collector supporting the aluminum electroplating of Al in chloroaluminate IL or coated with a thin seeding layer of Al film, can be used in AGDIBs instead of Al foil.[42] Figure 2a illustrates the impact of the $AlCl_3$:EMIMCl molar ratio (r) on the charge storage capacity of the chloroaluminate ionic liquid anolytes. For instance, the gravimetric charge storage capacities of the $AlCl_3$/EMIMCl ionic liquid are equal to 19 mAh g^{-1} and 48 mAh g^{-1} for $r=1.3$ and $r=2$, accordingly. Considering the fact that the highest molar ratio between $AlCl_3$ and EMIMCl that forms an IL is 2:1, which is limiting the capacity of $AlCl_3$/EMIMCl ionic liquid to only 48 mAh g^{-1}, in this work, we were driven to test $AlCl_3$-saturated ionic liquid formulation with an excess of $AlCl_3$ powder. Thus, while charging the battery, $AlCl_3$ precipitate can slowly dissolve in IL to maintain its acidity by forming $Al_2Cl_7^-$ ions, thus providing an additional contribution to the charge-storage capacity of anolyte as depicted in Figure 1. Corresponding redox reactions that take place upon the charge of AGDIB can be described as follows [Eqs. (1)–(3)]:
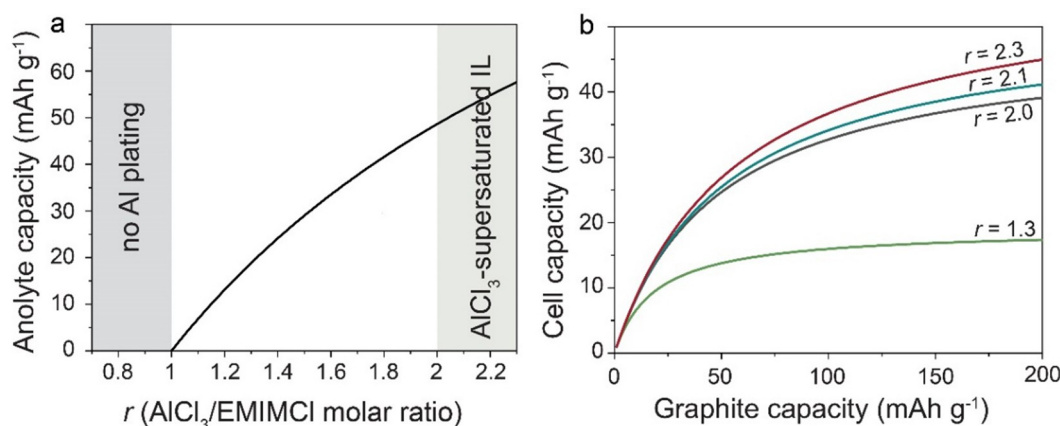
On the negative electrode:

$$4Al_2Cl_7^- + 3e^- \leftrightarrow 7AlCl_4^- + Al \tag{1}$$

$$AlCl_3 + AlCl_4^- \leftrightarrow Al_2Cl_7^- \tag{2}$$

On the positive electrode:

$$C + xAlCl_4^- \leftrightarrow C(AlCl_4)_x + xe^- \tag{3}$$

Hence, following the above-mentioned consideration, the theoretical capacities of $AlCl_3$-saturated IL anolytes with an excess of $AlCl_3$ can be increased, for instance, by up to ca. 52 and 58 mAh g^{-1} for $r=2.1$ and 2.3, accordingly. The latter improves the cell-level capacity of AGDIB of up to 36 and 39 mAh g^{-1}, respectively (assuming charge-storage capacity of graphite of ca. 120 mAh g^{-1}) as compared to IL formulation with $r=1.3$ or 2.0 [$C_{cell} = 16$ mAh g^{-1} ($r=1.3$); $C_{cell} = 34$ mAh g^{-1} ($r=2$), Figure 2b]. It should be noted, however, that an increase in r often leads to a concomitant decrease in graphite capacity and the average discharge voltage,[9,43] as is apparent from the electrochemical measurements, which will be discussed in the next section.
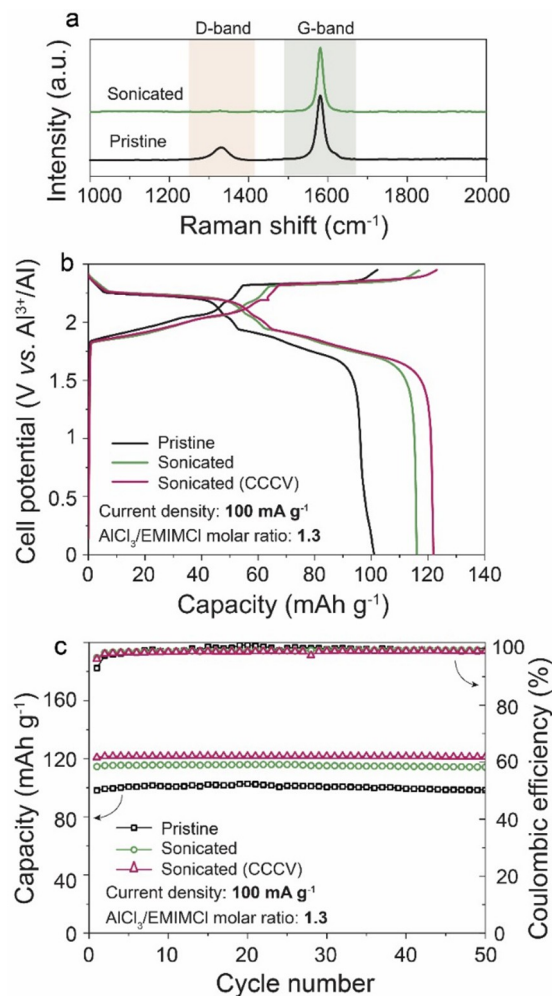

Figure 2. a) The charge-storage capacity of $AlCl_3$/EMIMCl anolyte versus its acidity (r). b) Comparison of the calculated cell-level capacities of AGDIBs comprising $AlCl_3$/EMIMCl anolyte of different acidities. The curves are computed from Eq. S22 published in the Supporting information of Ref. [49].

Electrochemical Performance of AGDIB Composed of Vein Graphite Cathode

Recent experimental endeavors have revealed that the major factors that govern the efficient uptake of $AlCl_4^-$ ions in the graphite are the flaky morphologies and high atomistic structural quality of graphite.[43,44,45,46] From this perspective, in this work, we were motivated to probe a unique form of highly crystalline graphite called vein graphite. This kind of graphite is found in veins and fissures of the rocks.[47,48] Due to the natural fluid-to-solid deposition process, vein graphite exists with a purity of up to 99.5% (percentage of the carbon in the form of graphite) in its natural state. In many applications, vein graphite offers superior performance compared to the natural graphite flakes produced from graphite ore since it has higher thermal and electrical conductivity, owing to its high degree of crystalline perfection.

Prior to carrying out AGDIB tests employing $AlCl_3$-saturated ionic liquid anolyte with an excess of $AlCl_3$ powder, the electrochemical performance of the vein graphite was assessed using the conventional ionic liquid formulation, that is, an $AlCl_3$:EMIMCl molar ratio of 1.3. We started with large commercial vein graphite (2.5–6 cm in lateral size), which was fragmentized by pestle in a mortar into smaller mm-sized particles (Figures S1 and S2). Afterward, we have tested the effect of the sonication-induced mechanical fragmentation of the vein graphite on their electrochemical performance. Pre-fragmented mm-sized vein graphite particles (0.2 g) were placed into a 4 ml glass vial with 3.5 ml ethanol and sonicated for 45 min (10% power) using Sonopuls ultrasonic homogenizer HD2200. Then, the sonicated graphite was washed three times with ethanol and dried in a vacuum at 80 °C for 12 h. Interestingly, sonication had a dual effect. On one side, it decreased the lateral flake size to ca. 80 μm (Figure S3). On the other side, it helped to reduce the amount of structurally disorder graphite as follows from the intensity decrease of the D band on Raman spectra of sonicated graphite as compared to the pristine sample (Figure 3a). Consequently, the sonication eventually lead to the considerable improvement of the charge-storage capacity of the graphite up to 120 mAh g^{-1} at a current density of 100 mAh g^{-1}. Moreover, this capacity could be increased even further while applying CCCV (constant current–constant voltage) charging protocol, which involves the combination of constant current and constant voltage (at 1.92 and 2.07 V, terminated at a current drop of 90%) charging steps (Figure 3b, c).
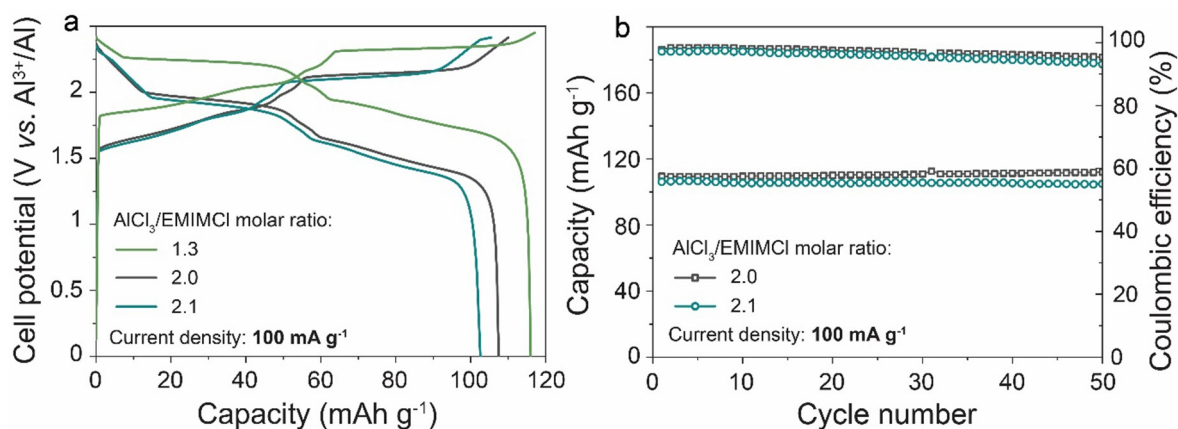
Having determined that the sonicated vein graphite flakes offer higher charge-storage capacities, we examined this form of graphite in combination with $AlCl_3$-saturated anolytes with an excess of $AlCl_3$ powder ($r=2.1$). ILs were prepared by slow mixing of EMIMCl solid powder and $AlCl_3$ granules in an argon-filled glovebox, following its heat-treatment at 150 °C for 10 min and the impregnation of the anolyte into the glass-fiber separator. At 150 °C, $AlCl_3$ was fully dissolved in IL anolyte. After assembly of batteries, an excess amount of $AlCl_3$ was crystallizing in the form of precipitate in the glass fiber separator.

Figure 3. a) Raman spectroscopy measurements of pristine and sonicated vein graphite flakes. b, c) Galvanostatic charge-discharge voltage curves and cyclic stability of pristine and sonicated vein graphite flakes measured without and with CCCV protocol at the current density of 100 mA g^{-1} using an anolyte with 1.3:1 ($AlCl_3$/EMIMCl) molar ratio.

Notably, although we have also attempted to prepare $AlCl_3$-saturated anolytes with $r=2.3$, at such a high $AlCl_3$/EMIMCl molar ratio $AlCl_3$ was not fully soluble in the IL even at a high temperature of 150 °C. Consequently, the electrochemical performance of vein graphite was performed, employing only IL with $r=2.1$. As illustrated in Figure 4a, the higher the acidity of chloroaluminate ionic liquid leads to lower voltage and capacity. The average discharge voltages and capacities at $r=1.3$, 2.0, and 2.1 were 1.99, 1.73, 1.71 V vs. Al^{3+}/Al, and 116, 108, and 103 mAh g^{-1}, respectively. However, the cycling stability tests of vein graphite measured with IL with $r=2.1$ show high capacity retention in excess of 105 mA g^{-1} for at least 50 cycles with a Coulombic efficiency of 93–97% (Figure 4b). We note that by the increasing r we observed a significant lowering of the Coulombic efficiency, which is associated with the intensified oxidation of the tungsten current collector in IL anolyte.[23,46,50]

These results suggest that the energy density of AGDIBs comprising the vein graphite cathode and IL chloroaluminate

Batteries & Supercaps

Communications
doi.org/10.1002/batt.202000289

**Chemistry
Europe**
European Chemical
Societies Publishing

Figure 4. a) Galvanostatic charge-discharge voltage curves of sonicated vein graphite flakes measured at a current density of 100 mA g^{-1} in AlCl$_3$:EMIMCl ionic liquid with $r=1.3$, 2.0, and 2.1. b) Cycling stability measurements of sonicated vein graphite flakes measured at a current density of 100 mA g^{-1} in AlCl$_3$/EMIMCl ionic liquid with $r=2.0$ and 2.1. Cycling stability measurements at higher currents of 500 mA g^{-1} are shown in Figure S4.

anolyte with $r=2.1$ can be as high as 59.1 Wh kg^{-1}, as estimated from the graphite capacity of 103 mAh g^{-1}, the anolyte capacity of 52 mAh g^{-1} and an average discharge voltage of 1.71 V. Importantly, although the capacity of graphite and the voltage of AGDIB comprising anolyte with $r=2$ were slightly higher than for $r=2.1$, the overall cell energy density at $r=2$ was lower, ca. 57.6 Wh kg^{-1}, due to the higher charge-storage capacity of the anolyte (48 mAh g^{-1} vs. 52 mAh g^{-1} for $r=2$ and 2.1). Also, for comparison, with the conventional formulation of this ionic liquid ($r=1.3$), the energy density of AGDIB is limited to at most 33 Wh kg^{-1}, with the graphite capacity of 116 mAh g^{-1} and the average discharge voltage of 1.99 V.

In summary, we have demonstrated a proof-of-concept of an AGDIB comprising an AlCl$_3$-saturated IL anolyte with an excess of AlCl$_3$ powder (AlCl$_3$:EMIMCl with the molar ratio of 2.1) to obtain high-energy densities up to 59.1 Wh kg^{-1}. The corresponding cathodic capacity was up to 103 mAh g^{-1}, and the average discharge voltage was 1.71 V. The AGDIB exhibited high-energy efficiencies (ca. 85%), on par with well-established battery technologies, such as lead-acid batteries (90%) and Li-ion batteries (90–95%). We suggest that future work should focus on the development of a new AGDIB cell design that allows achieving a homogeneous distribution of higher amounts of excess AlCl$_3$ within IL anolyte (with $r>2.1$). Furthermore, additional studies are needed to unravel the morphological and compositional evolution of excess AlCl$_3$ during electrochemical cycling.

Acknowledgements

Conflict of Interest

The authors declare no conflict of interest.

Keywords: graphite · aluminum · dual-ion battery · ionic liquid · energy density

[1] G. A. Elia, G. Greco, P. H. Kamm, F. García-Moreno, S. Raoux, R. Hahn, *Adv. Funct. Mater.* **2020**, *30*, 2003913.
[2] B. Craig, T. Schoetz, A. Cruden, C. Ponce de Leon, *Renewable Sustainable Energy Rev.* **2020**, *133*, 110100.
[3] K. Zhang, K. O. Kirlikovali, J. M. Suh, J.-W. Choi, H. W. Jang, R. S. Varma, O. K. Farha, M. Shokouhimehr, *ACS Appl. Mater. Interfaces* **2020**, *3*, 6019–6035.
[4] Y. Sui, C. Liu, R. C. Masse, Z. G. Neale, M. Atif, M. AlSalhi, G. Cao, *Energy Storage Mater.* **2020**, *25*, 1–32.
[5] G. A. Elia, K. V. Kravchyk, M. V. Kovalenko, J. Chacón, A. Holland, R. G. A. Wills, *J. Power Sources* **2021**, *481*, 228870.
[6] S. B. Patil, H.-J. Liao, D.-Y. Wang, *Phys. Chem. Chem. Phys.* **2020**, *22*, 24842–24855.
[7] K. V. Kravchyk, M. V. Kovalenko, *MRS Energy Sustain.* **2020**, *7*, E36.
[8] K. V. Kravchyk, M. V. Kovalenko, *Adv. Energy Mater.* **2020**, *10*, 2002151.
[9] M.-C. Lin, M. Gong, B. Lu, Y. Wu, D.-Y. Wang, M. Guan, M. Angell, C. Chen, J. Yang, B.-J. Hwang, H. Dai, *Nature* **2015**, *520*, 324.
[10] D.-Y. Wang, C.-Y. Wei, M.-C. Lin, C.-J. Pan, H.-L. Chou, H.-A. Chen, M. Gong, Y. Wu, C. Yuan, M. Angell, Y.-J. Hsieh, Y.-H. Chen, C.-Y. Wen, C.-W. Chen, B.-J. Hwang, C.-C. Chen, H. Dai, *Nat. Commun.* **2017**, *8*, 14283.
[11] F. Wu, H. Yang, Y. Bai, C. Wu, *Adv. Mater.* **2019**, *31*, 1806510.
[12] D. Muñoz-Torrero, J. Palma, R. Marcilla, E. Ventosa, *Dalton Trans.* **2019**, *48*, 9906–9911.
[13] D. Muñoz-Torrero, M. Anderson, J. Palma, R. Marcilla, E. Ventosa, *ChemElectroChem* **2019**, *6*, 2766–2770.
[14] J. H. Xu, D. E. Turney, A. L. Jadhav, R. J. Messinger, *ACS Appl. Mater. Interfaces* **2019**, *2*, 7799–7810.
[15] E. Zhang, J. Wang, B. Wang, X. Yu, H. Yang, B. Lu, *Energy Storage Mater.* **2019**, *23*, 72–78.
[16] Y. Hu, S. Debnath, H. Hu, B. Luo, X. Zhu, S. Wang, M. Hankel, D. J. Searles, L. Wang, *J. Mater. Chem. A* **2019**, *7*, 15123–15130.
[17] C. Liu, Z. Liu, Q. Li, H. Niu, C. Wang, Z. Wang, B. Gao, *J. Power Sources* **2019**, *438*, 226950.

[18] P. Bhauriyal, G. Bhattacharyya, K. S. Rawat, B. Pathak, *J. Phys. Chem. C* **2019**, *123*, 3959–3967.

[19] C. Liu, Z. Liu, H. Niu, C. Wang, Z. Wang, B. Gao, J. Liu, M. Taylor, *MethodsX* **2019**, *6*, 2374–2383.

[20] W.-L. Song, S. Li, G. Zhang, J. Tu, H.-S. Chen, S. Jiao, *Sustain. Energ. Fuels* **2019**, *3*, 3561–3568.

[21] X. Dong, H. Xu, H. Chen, L. Wang, J. Wang, W. Fang, C. Chen, M. Salman, Z. Xu, C. Gao, *Carbon* **2019**, *148*, 134–140.

[22] H. Huang, F. Zhou, X. Shi, J. Qin, Z. Zhang, X. Bao, Z.-S. Wu, *Energy Storage Mater.* **2019**, *23*, 664–669.

[23] J. Shi, J. Zhang, J. Guo, *ACS Energy Lett.* **2019**, *4*, 2124–2129.

[24] G. Greco, D. Tatchev, A. Hoell, M. Krumrey, S. Raoux, R. Hahn, G. A. Elia, *J. Mater. Chem. A* **2018**, *6*, 22673–22680.

[25] G. A. Elia, I. Hasa, G. Greco, T. Diemant, K. Marquardt, K. Hoeppner, R. J. Behm, A. Hoell, S. Passerini, R. Hahn, *J. Mater. Chem. A* **2017**, *5*, 9682–9690.

[26] G. A. Elia, N. A. Kyeremateng, K. Marquardt, R. Hahn, *Batteries Supercaps* **2019**, *2*, 83–90.

[27] H. Yang, H. Li, J. Li, Z. Sun, K. He, H.-M. Cheng, F. Li, *Angew. Chem. Int. Ed.* **2019**, *58*, 11978–11996.

[28] A. Zhou, L. Jiang, J. Yue, Y. Tong, Q. Zhang, Z. Lin, B. Liu, C. Wu, L. Suo, Y.-S. Hu, H. Li, L. Chen, *ACS Appl. Mater. Interfaces* **2019**, *11*, 41356–41362.

[29] K. V. Kravchyk, M. V. Kovalenko, *Commun. Chem.* **2020**, *3*, 120.

[30] K. V. Kravchyk, C. Seno, M. V. Kovalenko, *ACS Energy Lett.* **2020**, *5*, 545–549.

[31] K. Liang, L. Ju, S. Koul, A. Kushima, Y. Yang, *Adv. Energy Mater.* **2019**, *9*, 1802543.

[32] P. K. Lai, M. Skyllas-Kazacos, *Electrochim. Acta* **1987**, *32*, 1443–1449.

[33] Y. Chao-Cheng, *Mater. Chem. Phys.* **1994**, *37*, 355–361.

[34] Y. Zhao, T. J. VanderNoot, *Electrochim. Acta* **1997**, *42*, 3–13.

[35] S. Zein El Abedin, E. M. Moustafa, R. Hempelmann, H. Natter, F. Endres, *ChemPhysChem* **2006**, *7*, 1535–1543.

[36] T. Jiang, M. J. Chollier Brym, G. Dubé, A. Lasia, G. M. Brisard, *Surf. Coat. Technol.* **2006**, *201*, 1–9.

[37] T. Jiang, M. J. Chollier Brym, G. Dubé, A. Lasia, G. M. Brisard, *Surf. Coat. Technol.* **2006**, *201*, 10–18.

[38] H. M. A. Abood, A. P. Abbott, A. D. Ballantyne, K. S. Ryder, *Chem. Commun.* **2011**, *47*, 3523–3525.

[39] A. P. Abbott, R. C. Harris, Y.-T. Hsieh, K. S. Ryder, I. W. Sun, *Phys. Chem. Chem. Phys.* **2014**, *16*, 14675–14681.

[40] A. Bakkar, V. Neubert, *Electrochem. Commun.* **2015**, *51*, 113–116.

[41] Y. Fang, K. Yoshii, X. Jiang, X.-G. Sun, T. Tsuda, N. Mehio, S. Dai, *Electrochim. Acta* **2015**, *160*, 82–88.

[42] Q. Zhao, J. Zheng, Y. Deng, L. Archer, *J. Mater. Chem. A* **2020**, *8*, 23231–23238.

[43] K. V. Kravchyk, S. Wang, L. Piveteau, M. V. Kovalenko, *Chem. Mater.* **2017**, *29*, 4484–4492.

[44] S. Wang, K. V. Kravchyk, F. Krumeich, M. V. Kovalenko, *ACS Appl. Mater. Interfaces* **2017**, *9*, 28478–28485.

[45] P. Bhauriyal, A. Mahata, B. Pathak, *Phys. Chem. Chem. Phys.* **2017**, *19*, 7980–7989.

[46] S. Wang, K. V. Kravchyk, A. N. Filippin, U. Müller, A. N. Tiwari, S. Buecheler, M. I. Bodnarchuk, M. V. Kovalenko, *Adv. Sci.* **2018**, *5*, 1700712.

[47] F. J. Luque, J. M. Huizenga, E. Crespo-Feo, H. Wada, L. Ortega, J. F. Barrenechea, *Miner. Depos.* **2014**, *49*, 261–277.

[48] J. L. R. Touret, J. M. Huizenga, K. V. W. Kehelpannala, F. Piccoli, *Chem. Geol.* **2019**, *508*, 167–181.

[49] K. V. Kravchyk, M. V. Kovalenko, *Adv. Energy Mater.* **2019**, *9*, 1901749.

[50] C. Xu, S. Zhao, Y. Du, W. Zhang, P. Li, H. Jin, Y. Zhang, Z. Wang, J. Zhang, *ChemElectroChem* **2019**, *6*, 3350–3354.